chemengineering

MDPI

Article

Photocatalytic Reduction of Hexavalent Chromium with Nanosized TiO_2 in Presence of Formic Acid

Jahida Binte Islam [1,*], Mai Furukawa [1], Ikki Tateishi [2], Hideyuki Katsumata [1] and Satoshi Kaneco [1,2]

[1] Department of Chemistry for Materials, Graduate School of Engineering, Mie University, Mie, Japan; maif@chem.mie-u.ac.jp (M.F.); hidek@chem.mie-u.ac.jp (H.K.)

[2] Global Environment Center for Education & Research, Mie University, Mie, Japan; tateishi@gecer.mie-u.ac.jp (I.T.); kaneco@chem.mie-u.ac.jp (S.K.)

* Correspondence: jbislam07@gmail.com; Tel.: +81-59-231-9427

Received: 5 February 2019; Accepted: 29 March 2019; Published: 2 April 2019

Abstract: Nanosized titanium dioxide (TiO_2) nanoparticles were used for the photocatalytic reduction of hexavalent chromium in the presence of formic acid. The photoreduction of Cr(VI) in the absence of formic acid was quite slow. When formic acid was added in the chromium solution as the hole scavenger, a rapid photocatalytic reduction of Cr(VI) was observed, owing to the consumption of hole and the acceleration of the oxidation reaction. Furthermore, three commercial TiO_2 nanoparticles (AEROXIDE® P25; Ishihara Sangyo ST-01; FUJIFILM Wako Pure Chemical Corp.) were evaluated for the photoactivity of reduction of Cr(VI).

Keywords: photocatalytic reduction; hexavalent chromium; nanosized TiO_2; hole scavenger; formic acid

1. Introduction

Chromium (Cr) is a regulated metal in groundwater as a pollutant [1]. The Cr contamination has emanated from tanneries, dyeing, pigments, electroplating, metal finishing and so on [2]. The chromium occurs in the oxidation states +3 and +6 in the environment. The oxidation state and speciation of chromium are responsible for its toxicity in nature [3]. Cr(VI), with its carcinogenic and mutagenic effects on living organisms, is the most toxic, relatively within the chromium species [4]. Therefore, a significant stage in Cr(VI) pollution remediation is the reduction of highly toxic, soluble and easily migrant Cr(VI) to approximately one hundred times less toxic, easier coordinated and precipitated Cr (III).

Numerous chemical and physicochemical processes, such as ion exchange, chemical precipitation, coagulation, membrane process, reduction and adsorption, have been traditionally proposed [5–7]. Among these technologies, the heterogeneous photocatalytic reduction process has become one of the promising methods by virtue of cost-effectiveness, high catalytic performance and no secondary pollution [8].

Thus far, in various semiconductor oxides, titanium dioxide (TiO_2) has attracted enormous attention for widespread environmental applications, due to its low-cost, stability, nontoxicity, optical and electrical properties [9]. When nanosized TiO_2 particles are irradiated with UV light ($\lambda <$ 387 nm), photo-induced electrons are generated and excited from the valence bond (VB) to the conduction band (CB). While the photo-induced electrons are generally applied into reducing protons in water to evolve H_2 gas, in addition, these electrons can be used to remediate harmful contaminants by reducing hexavalent Cr to a trivalent. Normally, the photocatalytic reduction is more positive for the standard reduction potential of hexavalent Cr, compared with the conduction

band of the photocatalyst, though several hundred mVs of overpotential are frequently required owing to mass transfer, kinetic and ohmic losses [10].

Since the oxidation of water to oxygen is a kinetically slow process during the photocatalytic reduction of Cr(VI) to Cr(III), the conversion rate of Cr(VI) generally proceeds very slowly [11]. The addition of hole scavengers during the photoreduction of hexavalent chromium could greatly enhance the photocatalytic reduction of Cr [12,13]. First, it was reported by Sun et al. [14] that the addition of formic acid was very effective for the improvement of photocatalytic Cr reduction with P25 TiO_2. Next, Wang et al. [11] described that there was little positive effect of a formic acid scavenger on the reduction of hexavalent chromium in an aqueous solution using TiO_2, which was supplied from Zhoushan Nano Company (China). Therefore, in the present work, the photocatalytic reduction of hexavalent chromium with various commercial nanosized TiO_2 in the presence of formic acid was evaluated, and the photocatalytic activity of Cr reduction was discussed on the photocatalyst properties, such as the specific surface area and particle diameter.

2. Materials and Methods

2.1. Photocatalysts and Chemicals

Three commercial TiO_2 (AEROXIDE® P25; Ishihara Sangyo ST-01; FUJIFILM Wako Pure Chemical Corp., Osaka, Japan) was used as received, without further purification. Basic information is as follows, for AEROXIDE® P25: Anatase 75%, rutile 25%, specific surface area 50 $m^2 \cdot g^{-1}$, mean particle size 25 nm; for Ishihara Sangyo Kaisha, LTD, ST-01: Specific surface area 300 $m^2 \cdot g^{-1}$, mean particle size 7 nm; for FUJIFILM Wako Pure Chemical Corp., anatase form: Specific surface area 8.7 $m^2 \cdot g^{-1}$, mean particle size 230 nm [15]. Potassium dichromate, formic acid, sulfuric acid, acetone and 1,5-diphenylcarbazide were purchased from FUJIFILM Wako Pure Chemical Corp., and were of analytical reagent grade. A standard stock solution of Cr(VI) 1000 $\mu g \cdot mL^{-1}$ as $K_2Cr_2O_7$ was obtained from FUJIFILM Wako Pure Chemical Corp.

2.2. Photocatalytic Reduction of Cr(VI)

The Pyrex vessel reactor (inner capacity: 50 cm^3) was used for the photocatalytic reduction of hexavalent chromium ions in an aqueous solution. Typically, 20 mg of TiO_2 photocatalysts were added to 30 mL of 30 $\mu g \cdot mL^{-1}$ Cr(VI) aqueous solution in the reactor. Formic acid (0.30%) was added as the hole scavenger into the solution. The pH was set to 3. Before the illumination, the suspension was allowed to reach adsorption–desorption equilibrium with continuous and vigorous stirring for 30 min in the dark. During the irradiation, the suspensions were still under continuous stirring. A black light (Toshiba Lighting & Technology Corp., Tokyo, Japan, 15 W) was applied with a maximum emission of about 352 nm as the light source, which was positioned on the side of the reactor. The light intensity was measured by a digital UV intensity meter (USHIO, UIT-201) with a sensor (UV-365PD, 330~390 nm), and a value of 0.25 $mW \cdot cm^{-2}$. The samples, withdrawn at each time interval, were centrifuged at 10,000 rpm for 10 min and their supernatant was subjected to the analysis of Cr(VI).

2.3. Analysis of Hexavalent Chromium

The residual concentration of Cr(VI) was measured with the nesslerization method using a UV-visible spectrometry (AS ONE Corp., ASV11D) at λ_{max} of 540 nm, according to the standard method for the examination of water. First, a 1 mL portion of the solution was taken from the sample and was subjected to centrifugation (12,000 rpm) for 5 min. The supernatant (300 μL) was sampled. The solution (300 μL), 500 μL of sulfuric acid (2 $mol \cdot L^{-1}$) and 200 μL of 1,5-diphenyl carbazide (10 $g \cdot L^{-1}$) were transferred into a 25 mL volumetric flask and diluted with pure water.

3. Results and Discussion

3.1. Chromium(VI) Species with pH

Chromium (VI) species may be present in aqueous solution as chromate (CrO_4^{2-}), dichromate ($Cr_2O_7^{2-}$), hydrogen chromate ($HCrO_4^-$), dihydrogen chromate (chromic acid, H_2CrO_4), hydrogen dichromate ($HCr_2O_7^-$), trichromate ($Cr_3O_{10}^{2-}$) and tetrachromate ($Cr_4O_{13}^{2-}$). The last three ions ($HCr_2O_7^-$, $Cr_3O_{10}^{2-}$ and $Cr_4O_{13}^{2-}$) have been observed only in solutions of pH < 0 or at a chromium (VI) concentration greater than 1 mol·L^{-1} [16]. Tandon et al. [17] have presented the influence of pH on chromium (VI) species in solution and used the following equilibrium constant for describing chromium speciation equilibria.

$$H_2CrO_4 \rightleftarrows H^+ + HCrO_4^-, \qquad k_1 = 0.18 \tag{1}$$

$$HCrO_4^- \rightleftarrows H^+ + CrO_4^{2-}, \qquad k_2 = 3.2 \times 10^{-7} \tag{2}$$

$$2HCrO_4^- \rightleftarrows Cr_2O_7^{2-} + H_2O, \qquad k_3 = 98 \tag{3}$$

The total chromium (VI) concentration *C* can be expressed as follows:

$$C = [H_2CrO_4] + [HCrO_4^-] + [CrO_4^{2-}] + [Cr_2O_7^{2-}] \tag{4}$$

The concentration of H_2CrO_4, that is, $[H_2CrO_4]$, in a solution of pH and the total chromium (VI) concentration *C*, was estimated by soling the quadratic equation.

$$C = [H_2CrO_4] + \frac{k_1[H_2CrO_4]}{[H^+]} + \frac{k_1k_2[H_2CrO_4]}{[H^+]^2} + \frac{k_1^2k_3[H_2CrO_4]^2}{[H^+]^2} \tag{5}$$

The concentrations of Cr(VI) species can be derived from the following equations.

$$[HCrO_4^-] = \frac{k_1[H_2CrO_4]}{[H^+]} \tag{6}$$

$$[CrO_4^{2-}] = \frac{k_1k_2[H_2CrO_4]}{[H^+]^2} \tag{7}$$

$$[Cr_2O_7^{2-}] = \frac{k_1^2k_3[H_2CrO_4]^2}{[H^+]^2} \tag{8}$$

Because the initial concentration of Cr(VI) was 30 μg·mL^{-1} (0.483 mmol·L^{-1}) in the experiment, the total chromium (VI) concentration *C* was set to 0.1 mmol·L^{-1} for the estimation of the chromium (VI) species. The fractions of Cr(VI) species after the calculation with a computer are illustrated in Figure 1.

Diphenylcarbazide appears as a sensitive and specific color reaction with hexavalent chromium in mineral acid solution [18]. The pink colored chromophore is a chelate of chromium (III) and diphenylcarbazone. Diphenylcarbazone is produced and simultaneously combines with chromium when diphenylcarbazide is oxidized by hexavalent chromium [19]. The reaction may be speculated as:

$$CrO_4^{2-} + 3H_4L + 8H^+ = [Cr(III)(HL)_2]^+ + Cr^{3+} + H_2L + 8H_2O \tag{9}$$

where H_4L is diphenylcarbazide:

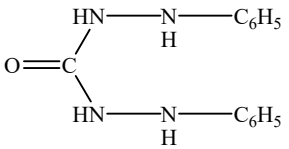

and H_2L is diphenylcarbazone:

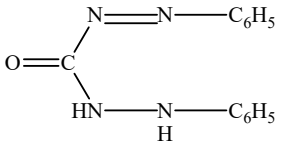

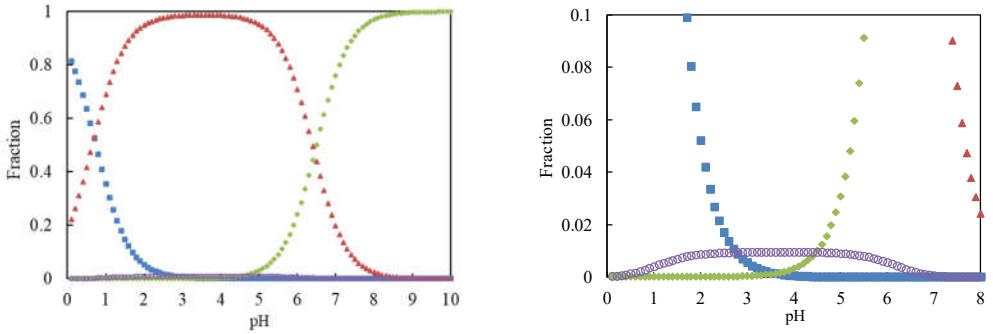

Figure 1. (**a**) Distribution of Cr(VI) species as functions of pH. Square (blue): H_2CrO_4; triangle (red): $HCrO_4^-$; diamond (green): CrO_4^{2-}; circle (purple): $Cr_2O_7^{2-}$; (**b**) Magnification for $Cr_2O_7^{2-}$ species.

The stability of the complex formation was evaluated for the determination of residual hexavalent chromium in the sample. The effect of the standing time on the absorbance of the resulted complex between 1,5-diphenylcarbazide and Cr(VI) was studied, as shown in Figure 2. From the graph, the absorbance of the complex was almost constant for 60 min. Therefore, the absorbance of the complex was measured after 5 min of standing time, since it was stable from 5 min.

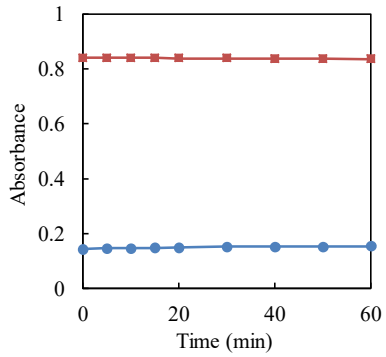

Figure 2. Effect of standing time on the absorbance of the complex between Cr(VI) and 1,5-diphenylcarbazide. Cr(VI) concentration: Circle (blue) 10 μg·mL^{-1}; square (red): 50 μg·mL^{-1}.

3.2. *Effect of Hole Scavengers*

First, the photocatalytic reduction of hexavalent chromium with TiO_2 in the aqueous solution was investigated in the absence of a hole scavenger. The results are shown in Figure 3. It was noticed that the photocatalytic reduction efficiency of Cr(VI) with TiO_2 without a hole scavenger was quite poor and approximately 50% of Cr(VI) remained in the solution after the photocatalytic treatment, for 3 hours.

Next, the influence of hole scavengers on the photocatalytic treatment of chromium (VI) with nanosized TiO_2 powders in the solution was investigated [20]. Ammonium formate and formic acid were checked as the hole scavengers. These chemical substances could not act as reducing agents. The results are illustrated in Figure 4. From the data, the addition of formic acid was very effective

for the photocatalytic reduction of Cr(VI) with nanosized TiO_2 powders in an aqueous solution. On the other hand, the occurrence of ammonium ions may disturb the consumption of the hole in the valence band in TiO_2 with the formate. Consequently, formic acid could be applied as the hole scavenger for the photocatalytic reduction of chromium (VI) with nanosized TiO_2 powders in water.

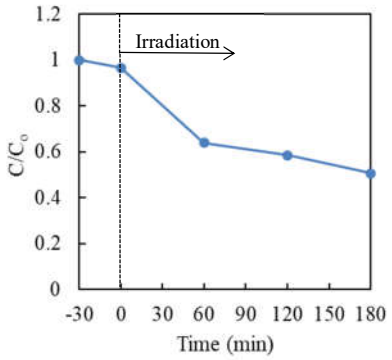

Figure 3. Effect of time on the photocatalytic reduction of Cr(VI) in aqueous solution with P25 TiO_2. Cr(VI) sample: 30 μg·mL^{-1} (30 mL); TiO_2: 20 mg (0.67 mg·mL^{-1}).

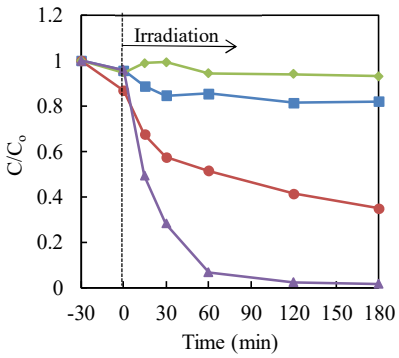

Figure 4. Effect of the hole scavengers on the photocatalytic reduction of Cr(VI) in aqueous solution with P25 TiO_2. Cr(VI) sample: 30 μg·mL^{-1} (30 mL); TiO_2: 20 mg (0.67 mg·mL^{-1}). Triangle (purple): TiO_2 with formic acid (3000 μg·mL^{-1}); circle (red): TiO_2 with ammonium formate (3000 μg·mL^{-1}); square (blue): formic acid (3000 μg·mL^{-1}) only; diamond (green): ammonium formate (3000 μg·mL^{-1}) only.

3.2. Effect of Commercial TiO_2 Type

The effect of different commercial TiO_2 on the photocatalytic treatment of Cr(VI) with TiO_2 nanoparticles in an aqueous solution, in the presence of a formic acid hole scavenger, was studied. The commercial TiO_2, AEROXIDE® P25, Ishihara Sangyo ST-01 and FUJIFILM Wako Pure Chemical Corp. were used for the evaluation of the photocatalytic activity. The data are shown in Figure 5. The maximum reduction rate of chromium (VI) was obtained with P25 TiO_2.

The relationship between the hexavalent chromium (VI) initial concentration Cr(VI) and initial reduction rate (r) can be explained by Langmuir-Hinshelwood model for the heterogeneous photocatalytic reduction process [21].

$$r = \frac{d[\mathrm{Cr(VI)}]}{d\mathrm{t}} = k\frac{K[\mathrm{Cr(VI)}]}{1 + K[\mathrm{Cr(VI)}]} \quad (10)$$

where k and K are the kinetic rate constant of the surface reaction and the Langmuir-Hinshelwood adsorption equilibrium constant, respectively. If $1 >> K[\mathrm{Cr(VI)}]$, that is, the Cr(VI) concentration is very low, Equation (10) can simplify to the pseudo-first-order kinetic law [22].

$$r = \frac{d[\mathrm{Cr(VI)}]}{dt} = kK[\mathrm{Cr(VI)}] = k_{obs}[\mathrm{Cr(VI)}] \quad (11)$$

where k_{obs} is the pseudo-first-order rate constant (min^{-1}).

The primary reduction reaction can be considered to follow pseudo-first-order kinetics, according to Equation (11). Integrating both sides in Equation (11) gives the following.

$$-\ln \frac{[\mathrm{Cr(VI)}]}{[\mathrm{Cr(VI)}]_0} = k_{obs} t \quad (12)$$

where $[Cr(VI)]_0$ is the initial Cr(VI) concentration and t is the irradiation time.

So as to confirm the speculation, $-\ln(C/C_0)$ was plotted as a function of the treatment time (irradiation time). Because the liner relations were obtained in Figure 6 as expected, the reduction kinetics of Cr(VI) solution could follow pseudo-first-order kinetics, which was consistent with the Langmuir-Hinshelwood model, resulting from the low coverage in the experimental concentration range (30 $\mu g \cdot mL^{-1}$). The kinetic parameters containing the rate constant, surface area-normalized rate constant, correlation coefficient and substrate half-life are presented in Table 1.

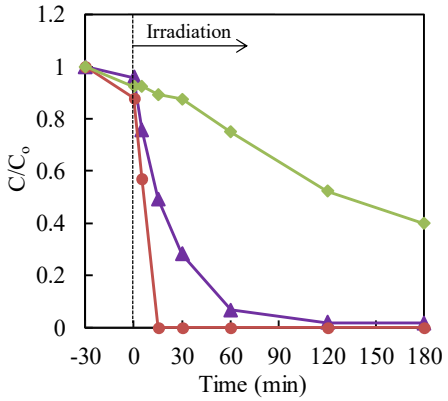

Figure 5. Effect of different commercial TiO_2 on the photocatalytic treatment of Cr(VI) with nanoparticles of TiO_2 in an aqueous solution, in the presence of formic acid hole scavenger. Cr(VI) sample: 30 $\mu g \cdot mL^{-1}$ (30 mL); TiO_2: 20 mg (0.67 $mg \cdot mL^{-1}$). Circle (red): Ishihara Sangyo ST-01; triangle (purple): AEROXIDE® P25TiO_2; diamond (green): FUJIFILM Wako Pure Chemical Corp.

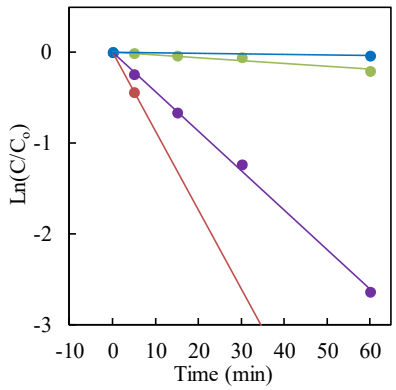

Figure 6. $-\ln(C/C_0)$ versus irradiation time. Cr(VI) sample: 30 $\mu g \cdot mL^{-1}$ (30 mL); TiO_2: 20 mg (0.67 $mg \cdot mL^{-1}$). With formic acid hole scavenger: red for Ishihara Sangyo ST-01; purple for AEROXIDE® P25TiO_2; green for FUJIFILM Wako Pure Chemical Corp. Without hole scavenger: blue for AEROXIDE® P25TiO_2.

The maximum photocatalytic reduction rate for hexavalent chromium was observed with Ishihara Sangyo ST-01 nanosized TiO_2 (mean particle size 7 nm). However, the highest rate constant, based on the specific surface area normalization, was obtained with AEROXIDE® P25 TiO_2. Therefore, it was concluded from the surface area-normalized rate constant that the surface area of TiO_2 can play a significant role in the photocatalytic activity for Cr(VI) reduction in the presence of a formic acid hole scavenger.

Table 1. Kinetic parameters for the photocatalytic reduction of Cr(VI).

Commercial TiO_2	Specific surface area ($m^2 \cdot g^{-1}$)	k_{obs} (min^{-1})	Surface area-normalized k_{sur} ($m^2 \cdot min^{-1} \cdot g^{-1}$)	R^2	$t_{1/2}$ (min)
FUJIFILM Wako	8.7	0.0031	3.6×10^{-4}	0.999	224
AEROXIDE® P25	50	0.043	8.6×10^{-4}	0.998	16.1
Ishihara ST-01	300	0.087	2.9×10^{-4}	0.999	7.97
P25 (Without scavenger)	50	0.00058	0.12×10^{-4}	0.999	1190

k_{obs}: Pseudo-first-order rate constant; surface area-normalized k_{sur}: k_{obs}/specific surface area; R^2: Correlation coefficient; $t_{1/2}$: substrate half-life.

3.2. Reaction Mechanism

The proposed mechanism for the photocatalytic reduction of hexavalent chromium on nanosized TiO_2 in the presence of formic acid is illustrated in Figure 7. The nanosized TiO_2 with a bandgap of 3.2 eV can absorb the photons efficiently and be excited to form electrons in the conduction band (CB) and holes in the valance band (VB) under the UV irradiation.

Because the point of zero charge (pzc) of the TiO_2 particle is approximately equal to six as Ti^{IV}–OH [23]. This means that, when the pH is lower than this value, the TiO_2 surface becomes positively charged as Ti^{IV}–OH_2^+. From the estimation of Cr(VI) species as the function of pH, the main chemical species for hexavalent chromium at pH 3 is $HCrO_4^-$. Owing to the electrostatic attraction between $HCrO_4^-$ species and nanosized TiO_2 with a relatively large surface area, as well as the facilitation of the proton under acidic conditions, adsorbed Cr(VI) on the surface of TiO_2 can be immediately reacted with electrons and be reduced to Cr(III). Because of the presence of formic acid, the hydroxyl radical (•OH), which is produced from the holes and OH^-, is able to be captured by formic acid. This will produce reactive $\bullet CO_2^-$, which has a relatively negative redox potential, $E^0(\bullet CO_2^-/CO_2) = -1.9$ V vs. NHE [24,25], compared with the redox potential for Cr(VI), $E^0(HCrO_4^-/Cr^{3+}) = 1.35$ V vs. NHE [26].

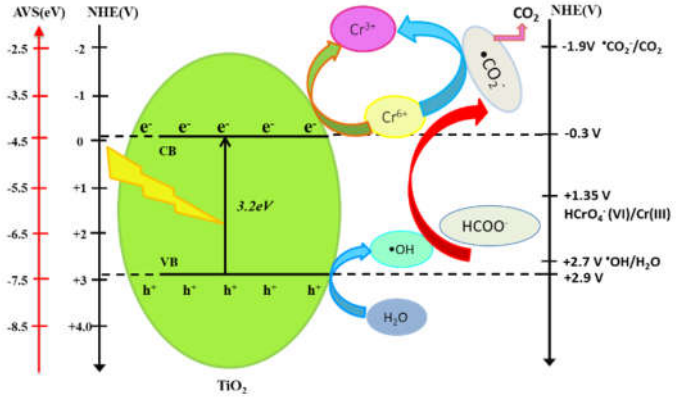

Figure 7. Reaction mechanism for the photocatalytic reduction of Cr(VI) with TiO_2 in the presence of formic acid.

$$TiO_2 + h\nu \rightarrow TiO_2 (e_{CB}^- + h_{VB}^+) \quad (13)$$

$$H_2O + h_{VB}^+ \rightarrow \bullet OH + H^+ \quad (14)$$

$$HCrO_4^- + 7H^+ + 3e_{CB}^- \rightarrow Cr^{3+} + 4H_2O \quad (15)$$

$$HCOOH + \bullet OH \rightarrow \bullet CO_2^- + H_3O^+ \quad (16)$$

$$HCrO_4^- + \bullet CO_2^- + 5H^+ \rightarrow Cr^{3+} + CO_2 + 3H_2O \quad (17)$$

In the present case, formic acid provided a multifunctional role in accelerating the separation of the holes and electrons, which was advantageous to the photocatalytic activity of nanosized TiO_2 and produced reactive radicals ($\bullet CO_2^-$). Hence, Cr(VI) can be reduced to trivalent chromium with nanosized TiO_2 effectively. In the present work, the surface area of TiO_2 may become an important factor in the photocatalytic activity for reducing hexavalent chromium in the presence of a formic acid hole scavenger.

4. Conclusions

The photocatalytic reduction of hexavalent chromium with nanosized TiO_2 nanoparticles in the presence of formic acid was investigated. The addition of the hole scavenger, formic acid, was very effective for the enhanced photocatalytic reduction of Cr(VI) on nanosized TiO_2 in an aqueous solution. Furthermore, the influence of different commercial TiO_2 on the photocatalytic treatment of Cr(VI) with nanosized TiO_2 in an aqueous solution, containing formic acid, was checked. As a consequence, the photocatalytic reduction of hexavalent chromium with Ishihara Sangyo ST-01 nanosized TiO_2 gave better efficiencies, due to the specific surface area.

Author Contributions: J.B.I. and S.K. conceived and designed the experiments; J.B.I. performed the experiments and wrote the paper; I.T., M.F. and H.K. analyzed the results and advised the project.

Funding: The present research was partly supported by Grant-in-Aid for Scientific Research (C) 15K00602 from the Ministry of Education, Culture, Sports, Science, and Technology of Japan.

Acknowledgments: All experiments were conducted at Mie University. Any opinions, findings, conclusions or recommendations expressed in this paper are those of the authors and do not necessarily reflect the view of the supporting organizations.

Conflicts of Interest: The authors declare no conflict of interest.

References

1. Korak, J.A.; Huggins, R.; Arias-Paic, P. Regeneration of Pilot-Scale Ion Exchange Columns for Hexavalent Chromium Removal. *Water Res*. **2017**, *118*, 141–151, doi:10.1016/j.watres.2017.03.018.
2. Du, X.D.; Yi, X.H.; Wang, P.; Zheng, W.; Deng, J.; Wang, C.C. Robust photocatalytic Reduction of Cr(VI) on UiO-66-NH2(Zr/Hf) Metal-Organic Framework Membrane Under Sunlight Irradiation. *Chem. Eng. J.* **2019**, *356*, 393–399, doi:10.1016/j.cej.2018.09.084.
3. Siboni, M.S.; Farroki, M.; Soltani, R.D.C.; Khataee, A.; Tajassosi, S. Photocatalytic Reduction of Hexavalent Chromium over ZnO Nanorods Immobilized on Kaolin. *Ind. Eng. Chem. Res.* **2014**, *53*, 1079–1087, doi:10.1021/ie4032583.
4. Shih, Y.J.; Chen, C.W.; Hsia, K.F.; Dong, C.D. Granulation for Extended-Release of Nanoscale Zero-Valent Iron Exemplified by Hexavalent Chromium Reduction in Aqueous Solution. *Sep. Purif. Technol.* **2015**, *156*, 1073–1081, doi:10.1016/j.seppur.2015.10.043.
5. Mohan, D.; Pittman, C.U., Jr. Activated Carbons and Low Cost Adsorbents for Remediation of Tri- and Hexavalent Chromium from Water. *J. Hazard. Mater*. **2006**, *137*, 762–811, doi:10.1016/j.jhazmat.2006.06.060.
6. Mohan, D.; Rajput, S.; Singh, V.K.; Steele, P.H.; Pittman, C.U., Jr. Modeling and Evaluation of Chromium Remediation from Water Using Low Cost Bio-Char, a Green Adsorbent. *J. Hazard. Mater*. **2011**, *188*, 319–333, doi:10.1016/j.jhazmat.2011.01.127.
7. Di Natale, F.; Erto, A.; Lancia, A.; Musmarra, D. Equilibrium and Dynamic Study on Hexavalent Chromium Adsorption onto Activated Carbon. *J. Hazard. Mater*. **2015**, *281*, 47–55, doi:10.1016/j.jhazmat.2014.07.072.
8. Qi, H.; Wang, S.; W.; Liu, H.; Gao, Y.; Wang, T.; Huang, Y. Synthesis of an Organic–Inorganic Polypyrrole/Titanium(IV) Biphosphate Hybrid for Cr(VI) Removal. *J. Mol. Liq.* **2016**, *215*, 402–409, doi:10.1016/j.molliq.2015.12.060.
9. Joubani, M.N.; Siboni, M.S.; Yang, J.K.; Gholami, M.; Farzadkia, M. Photocatalytic Reduction of Hexavalent Chromium with Illuminated ZnO/TiO_2 Composite. *J. Ind. Eng. Chem*. **2015**, *22*, 317–323, doi:10.1016/j.jiec.2014.07.025.

10. Cheng, Q.; Wang, C.; Doudrick, K.; Chan, C.K. Hexavalent Chromium Removal Using Metal Oxide Photocatalysts. *Appl. Catal. B* **2015**, *176–177*, 740–748, doi:10.1016/j.apcatb.2015.04.047.
11. Wang, N.; Zhu, L.; Deng, K.; She, Y.; Yu, Y.; Tang, H. Visible Light Photocatalytic Reduction of Cr(VI) on TiO_2 in Situ Modified with Small Molecular Weight Organic Acids. *Appl. Catal. B* **2010**, *95*, 400–407, doi:10.1016/j.apcatb.2010.01.019.
12. Testa, J.J.; Grela, M.A.; Litter, M.I. Heterogeneous Photocatalytic Reduction of Chromium (VI) over TiO_2 Particles in the Presence of Oxalate: Involvement of Cr(V) Species. *Environ. Sci. Technol*. **2004**, *38*, 1589–1594, doi:10.1021/es0346532.
13. Yang, J.K.; Lee, S.M. Removal of Cr(VI) and Humic Acid by Using TiO_2 Photocatalysis. *Chemosphere* **2006**, *63*, 1677–1684, doi:10.1016/j.chemosphere.2005.10.005.
14. Sun, B.; Reddy, E.P.; Smirniotis, P.G. Visible Light Cr(VI) Reduction and Organic Chemical Oxidation by TiO_2 Photocatalysis. *Environ. Sci. Technol.* **2005**, *39*, 6251–6259, doi:10.1021/es0480872.
15. Kaneco, S.; Kurimoto, H.; Ohta, K.; Mizuno, T.; Saji, A. Photocatalytic Reduction of CO_2 Using TiO_2 Powders in Liquid CO_2 Medium. *J. Photochem. Photobiol. A Chem.* **1997**, *109*, 59–63, doi:10.1016/S1010-6030(97)00107-X.
16. Szabó, M.; Kalmár, J.; Ditrói, T.; Bellér, G.; Lente, G.; Simic, N.; Fábián, I. Equilibria and Kinetics of Chromium(VI) Speciation in Aqueous Solution—A Comprehensive Study from pH 2 to 11. *Inorg. Chim. Acta* **2018**, *472*, 295–301, doi:10.1016/j.ica.2017.05.038.
17. Tandon, R.K.; Crisp, P.T.; Ellis, J.; Baker, R.S. Effect of pH on Chromium(VI) Species in Solution. *Talanta* **1984**, *31*, 227–228, doi:10.1016/0039-9140(84)80059-4.
18. Gardner, M.; Comber, S. Determination of Trace Concentration of Hexavalent Chromium. *Analyst* **2002**, *127*, 153–156, doi:10.1039/b109374f.
19. Duffy, G.; Maguire, I.; Heery, B.; Gers, P.; Ducrée, J.; Regan, F. ChromiSense: A Colourimetric Lab-on-a-Disc Sensor for Chromium Speciation in Water. *Talanta* **2018**, *178*, 392–399, doi:10.1016/j.talanta.2017.09.066.
20. Yang, J.K.; Lee, S.M.; Siboni, M.S. Effect of Different Types of Organic Compounds on the Photocatalytic Reduction of Cr(VI). *Environ. Technol*. **2012**, *33*, 2027–2032, doi:10.1080/09593330.2012.655325.
21. Turchi, C.S.; Ollis, D.E. Photocatalytic Degradation of Organic Water Contaminants: Mechanisms Involving Hydroxyl Radical Attack. *J. Catal.* **1990**, *122*, 178–192, doi:10.1016/0021-9517(90)90269-P.
22. Sofi, F.A.; Majid, K.; Mehraj, O. The Visible Light Driven Copper Based Metal-Organic-Framework Heterojunction:HKUST-1@Ag-Ag_3PO_4 for Plasmon Enhanced Visible Light Photocatalysis. *J. Alloys Compd.* **2018**, *737*, 798–808, doi:10.1016/j.jallcom.2017.12.141.
23. Samad, A.; Ahsan, S.; Tateshi, T.; Furukawa, M.; Katsumata, H.; Suzuki, T.; Kaneco, S. Indirect Photocatalytic Reduction of Arsenate to Arsenite in Aqueous Solution with TiO_2 in the Presence of Hole Scavengers. *Chin. J. Chem. Eng*. **2018**, *26*, 529–533, doi:10.1016/j.cjche.2017.05.019.
24. Shaban, Y.A.; Maradny, A.A.E.; Farawati, R.K.A. Photocatalytic Reduction of Nitrate in Seawater Using C/TiO_2 nanoparticles. *J. Photochem. Photobiol. A Chem.* **2016**, *328*, 114–121, doi:10.1016/j.jphotochem.2016.05.018.
25. Xu, Q.; Li, R.; Wang, C.; Yuan, D. Visible-Light Photocatalytic Reduction of Cr(Ⅵ) Using Nano-Sized Delafossite ($CuFeO_2$) Synthesized by Hydrothermal Method. *J. Alloys Compd*. **2017**, *723*, 441–447, doi:10.1016/j.jallcom.2017.06.243.
26. Wang, L.; Lia, X.; Tenga, W.; Zhaoa, Q.; Shi, Y.; Yue, R.; Chen, Y. Efficient Photocatalytic Reduction of Aqueous Cr(VI) over Flower-like $SnIn_4S_8$ Microspheres under Visible Light Illumination. *J. Hazard. Mater*. **2013**, *244–245*, 681–688, doi:10.1016/j.jhazmat.2012.10.062.